Biodegradable Polymeric Micro-Nanofibers by Electrospinning of Polyester/Polyether Block Copolymers

N. Detta,[1] A. A. El-Fattah,[1] E. Chiellini,[1] P. Walkenström,[2] P. Gatenholm[3]

[1]*Laboratory of Bioactive Polymeric Materials for Biomedical and Environmental Applications UdR-INSTM, Department of Chemistry and Industrial Chemistry, University of Pisa, 56100 Pisa, Italy*
[2]*IFP Research AB, P.O. Box 104, SE-431 22 Mölndal, Sweden*
[3]*Biopolymer Technology, Department of Chemical and Biological Engineering, Chalmers University of Technology, SE-412 96 Gothenburg, Sweden*

Received 6 July 2007; accepted 13 October 2007
DOI 10.1002/app.28640
Published online 9 July 2008 in Wiley InterScience (www.interscience.wiley.com).

ABSTRACT: Two block copolymers consisting of biodegradable segments of poly(ethylene glycol) (PEG) and poly(ε-caprolactone) (PCL) with slight different lengths of soft hydrophilic segments (PEG) and molecular weight were produced. The copolymer with shorter PEG segments and higher molecular weight was named copolymer A, while the other copolymer B. Both copolymers were dissolved in dichloromethane at the same concentration (5% w/v) and electrospun. Different combinations of spinning voltage (SV) and distance needle to collector were used. Electrospun A copolymer showed curly and uniform fibers with an average diameter of 2 μm, while B copolymer fibers were straight, uneven, and much thinner (submicrometric). In the latter case, fiber bundles and beads were also present. Viscosity measurements on the solutions before spinning showed a viscosity of 13.0 mPa s for A copolymer solution and 5.5 mPa s for B copolymer. The mechanical properties on dog-bone shaped samples from the electrospun material evidenced that A copolymer had much higher stress and elongation at break but approximately the same elastic modulus as compared to B copolymer. Fiber morphology and mechanical properties of electrospun block copolymers are deeply influenced by different amount and length of soft and hard segments, and block copolymers can be the best suited systems to fit several applications because of the broad range of properties they show upon changing the composition ratio and molecular weight of components. © 2008 Wiley Periodicals, Inc. J Appl Polym Sci 110: 253–261, 2008

Key words: biodegradable; block copolymers; structure–property relations; polyesters; polyethers

INTRODUCTION

Electrospinning is a technique that uses an applied electric field imposed on a polymer solution or melt, to produce nonwoven webs with high porosity, high surface area, and very fine fibers (50 nm to few microns) thus with one or two orders of magnitude finer than fibers produced by conventional extrusion techniques.[1–8] The electrospinning process takes advantage from the continuity of the process (possibility of high volume production), no loss of material, and the extreme simplicity of the required equipment, which is composed of only three major components: a high-voltage power supply (usually DC), a spinneret (a metallic needle on which the high voltage is applied), and a collector (a metallic sheet or metallic tube, grounded or connected to a power supply with opposite sign). The spinneret is connected to a syringe in which the polymer melt or solution is hosted and can be fed through the spinneret at a constant rate by means of a syringe pump with a selected needle orifice.[9]

Poly(ethylene glycol) (PEG) and poly(ε-caprolactone) (PCL) are widely used as biodegradable–biocompatible polymers in the biomedical field, both as homopolymers[10–13] and as relevant block copolymers, in which PEG constitutes the soft hydrophilic segment and PCL the relatively hard hydrophobic one. The PEG-PCL copolymers are actually investigated as drug carrier or imaging agent in the form of nanoparticles[14,15] and as innovative air filtration media, drug-delivery systems, or for other biomedical applications, in general, in the form of nano-nonwovens produced by electrospinning.[11] As known, polymers chemical composition and morphology influence the bulk properties (rheological behavior, mechanical properties). Block copolymers are of particular interest, because the combination of the single components can be balanced by using suitable molecular weights and amount of the coupled segments to obtain the characteristics required for the desired application.[16–20] The mechanical properties are, in

Correspondence to: E. Chiellini (emochie@dcci.unipi.it).
Contract grant sponsor: NoE Expertissues; contract grant number: NMP3-CT 2004-500328.

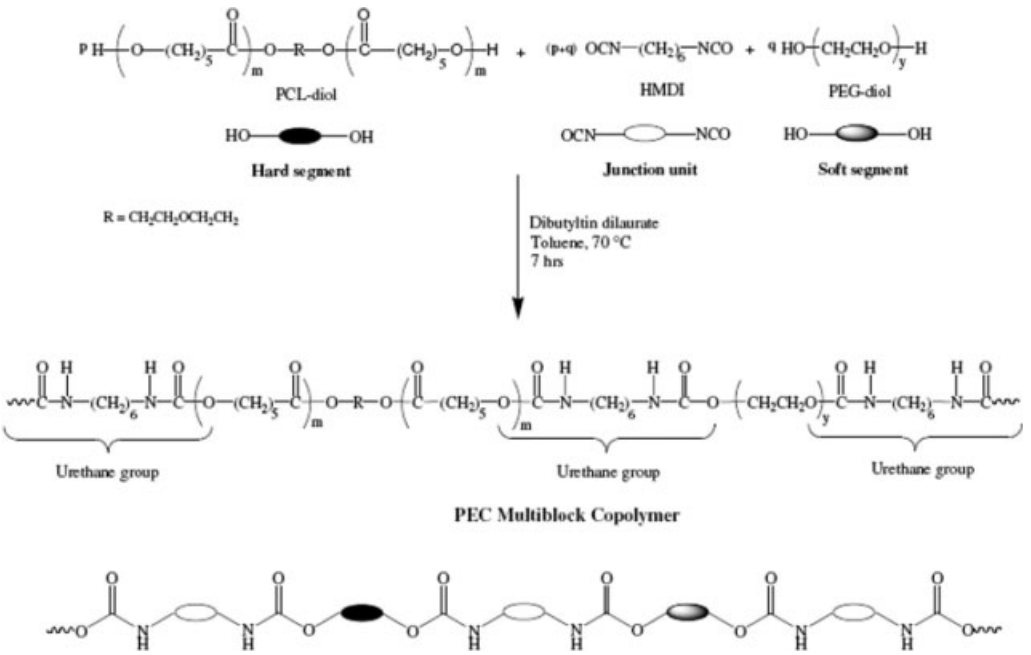

Scheme 1 Schematic synthesis pathway of PEC multiblock copolymers.

particular, an issue that has to be often faced when a material is implanted in the human body as temporary (e.g., bioerodible–bioeliminable scaffold) or permanent (e.g. long lasting prostheses) support or is designed to be in contact with human tissues just during a specific process (e.g. hemodialysis filters and assistance medical devices). In the case of a biodegradable scaffold, its mechanical properties decay as a consequence of degradation (whose rate depends upon chemical structure and morphology), while they increase in the new forming tissue as more and more extracellular matrix is deposited. Therefore, a perfect balance between the two contemporary antagonist processes is required.

Electrospun nanofibers are attractive as scaffolds for tissue engineering applications, because of their interconnected, three-dimensional porous structure that may be designed to mimic the morphology of the extracellular matrix (ECM).[12,21] Electrospun materials have already proven to be useful in the medical field for vascular grafts and prosthetic blood vessels, as well as for filtration applications.[22–25] Biodegradable–biocompatible polymeric materials are thought to be the best suited system for scaffold fabrication in tissue engineering, as they can provide the healing tissue with initial strength and degrade at a certain rate, letting the load to be carried gradually by the new forming ECM. The scaffold serves as a three-dimensional template for initial cell attachment and subsequent tissue formation both *in vitro* and *in vivo* and provides the necessary support for cells to attach, proliferate, and maintain their differentiated function. Its architecture defines the ultimate shape of the new grown soft or hard tissue.[26]

In this article, electrospinning of two PEG-PCL block copolymers with different molecular weight, amount of the components, and soft segments length is described. Solution viscosity test, SEM imaging and mechanical testing of the nonwoven sheets are performed to correlate chemical structure, electrospinning parameters, fiber morphology, and mechanical properties.

EXPERIMENTAL

Materials

Poly(ether–ester)urethane multiblock copolymers were synthesized by one-step condensation reaction in solution by coupling PCL-diol and PEG-diol with stoichiometric amounts of 1,6-hexamethylene diisocyanate (HMDI) as a chain extender according to a procedure described elsewhere (article in preparation). The selected hydroxylated prepolymers were dissolved in dry dichloromethane to give a concentrated solution (15% w/v) in the presence of equivalent amounts of HMDI, to which dibutyltin dilaurate (0.5% w/w), as a catalyst, was added. The reaction mixtures were allowed to react for 7 h at 70°C (Scheme 1). The copolymers were separated by precipitating the reaction mixture in excess of low-boiling petroleum ether. The isolated copolymers were purified by dissolution in chloroform and reprecipitation in diethyl ether, and finally dried under vacuum at room temperature for at least 48 h. Table I

TABLE I
Chemical Compositions, Molecular Weights, and Thermal Characteristics of the Poly(ether–ester–urethane)s Synthesized from PEG and PCL-Diol with HMDI

	M_n		Copolymer compositions[a] (wt %)						
Sample code	PEG-diol	PCL-diol	PEG-diol	PCL-diol	HMDI	M_w[b] (g/mol)	M_w/M_n[b]	T_g[c] (°C)	T_m[c] (°C)
A	2000	2000	44.8 (48.6)[d]	47.4 (51.4)	7.8 (100)	149,780	4.27	−49.1	50.0
B	4600	2000	77.8 (65.5)	17.8 (34.5)	4.4 (100)	105,470	3.46	−49.1	52.6

[a] Determined from ^{1}HNMR spectra.
[b] Determined from GPC in chloroform.
[c] Determined from DSC.
[d] Values in parentheses indicate mol %.

lists the chemical compositions, molecular weights, and thermal characteristics of the two prepared poly(ether–ester–urethane)s.

Methods

Electrospinning

Copolymers A and B were dissolved in dichloromethane at a concentration of 5% w/v. To guarantee the complete dissolution of the polymer in the solvent, the solutions were stirred, at medium velocity, for ~ 24 h. The solution containing copolymer A had a clear appearance while the one containing copolymer B was characterized by a milky consistence. The polymer solutions were electrospun from a 5-mL syringe with a blunt needle of 0.9-mm inner diameter. The flow rate was maintained at 5.5 mL/h using a synchronous motor (Clas Ohlson, 230 V, 3 W, 1 rpm) [Class Ohlson AB, Gothenburg/Sweden] as a pump. The high voltage was provided by a direct current power supply from Gamma High Voltage, USA. The electronic potential was applied to the needle through the tip of the voltage supply lead cable, and the fibers were collected onto a grounded aluminum foil. The samples were electrospun under several different combinations of the parameters "spinning voltage (SV)" and "distance needle to collector (DTC)," varying the SV between 15 and 30 kV and the DTC between 15 and 30 cm.

Rheology

Viscosity measurements on the 5% w/v concentration solutions were carried out at room temperature just before electrospinning by using a RHEOMAT-30 Contraves viscosimeter, based on two coaxial cylinders. Under fume hood, the space between the cylinders was filled with ~ 26 mL of the solution, and the external cylinder was rotating under constant velocity resulting in a shear rate at the wall of 375 s^{-1}. The value of shear viscosity was read on a graduate scale as percentage viscosity (η%) and, to obtain the corresponding value in mPa s, η% was multiplied by a factor of conversion given by the instrument manual, depending upon the rotational velocity of the cylinder. A preliminary measurement was performed to set the zero value of the scale when the cylinder was not rotating. Three measurements were performed on each of the two solutions and the shear viscosity obtained as average value.

Scanning electron microscopy

The microstructure of the electrospun fiber mats produced was analyzed by means of a scanning electron microscope (ZEISS DSM940A). First, squared samples of 5 mm × 5 mm were cut with a scalpel and retained on the aluminum foil to facilitate handling. After cutting, the samples were stuck on cylindrical aluminum holders using a Pelco® Colloidal Silver Liquid provided by Ted Pella, Inc. All specimens were sputter-coated (Edwards Sputter Coater S150B) with gold particles for 1 min, at a voltage of 0.1 kV and a current of 20 mA, and then analyzed upon setting into the SEM chamber. The accelerating voltage of the electron beam was 10 kV and images at different magnification were acquired from the signal of a secondary electrons detector.

Mechanical behavior

The tensile properties of the nonwoven webs were obtained using an INSTRON 1122 testing machine. The test was performed at 20°C and 65% of relative humidity on dog-bone shaped samples (6 cm in total length; 4 cm long and 1 cm wide in the central part). The thickness of the samples was measured at several points, and the average value was used as the thickness of each sample. The loading area was simply calculated by multiplying the width of the central part by the thickness. The specimens were placed between two holders, and paper tape was applied in the inner parts of the holders to provide better grip. The specimens were then pulled at a constant crosshead speed of 10 mm/min until failure, and the data of force versus elongation were acquired by the software. These data were transferred into an Excel file and the stress–strain curves

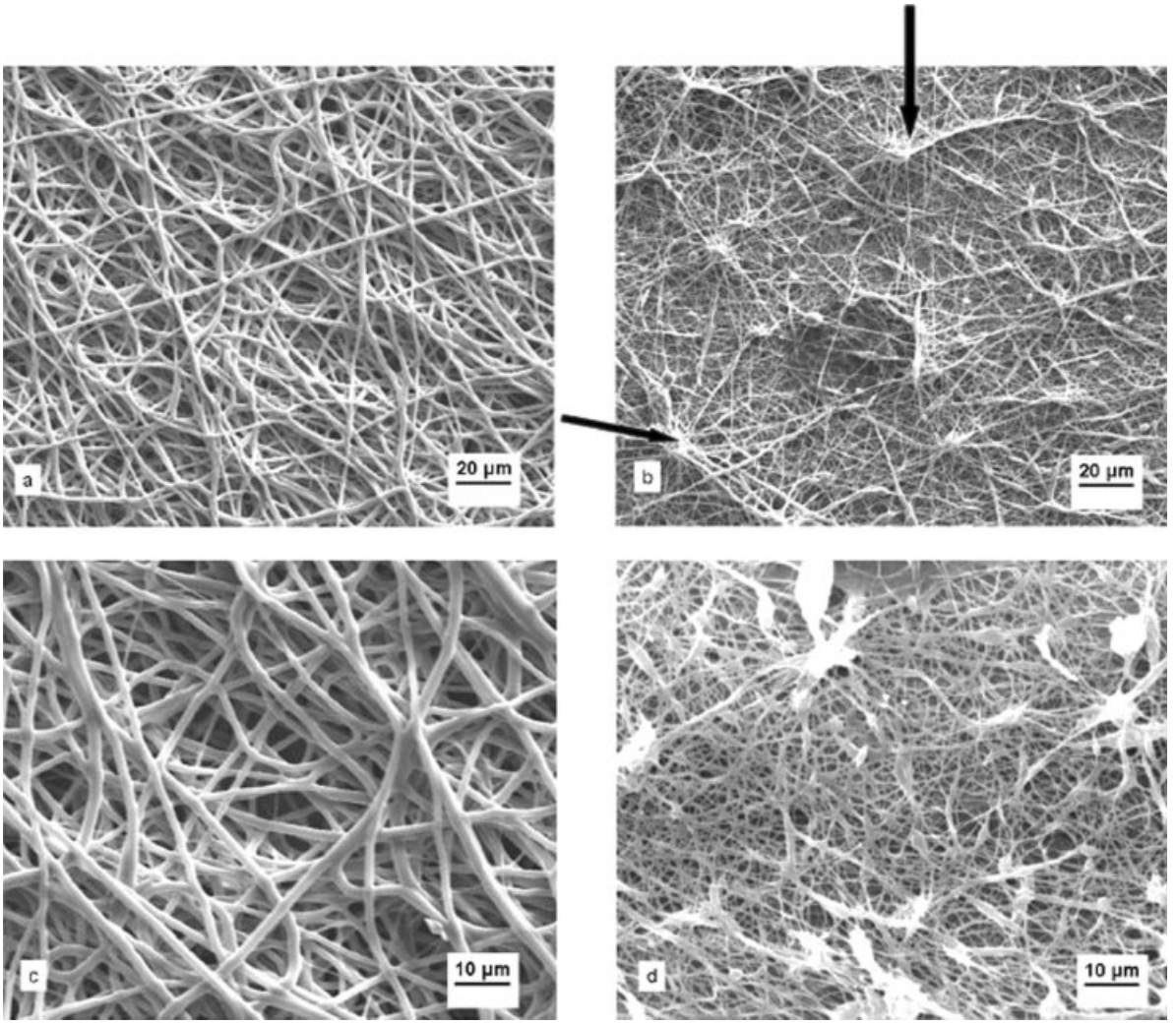

Figure 1 SEM images of electrospun fibers at a spinning voltage of 15 kV and a DTC of 15 cm. (a) A copolymer, ×500; (b) B copolymer, ×500; (c) A copolymer, ×1000; (d) B copolymer, ×1000.

were created in SigmaPlot 2000. Values of ultimate tensile strength and deformation at break were simply read from the diagram while the elastic region of the curves was interpolated with a linear regression function, whose angular coefficient represented the elastic modulus.

RESULTS AND DISCUSSION

Comparison between copolymer A and B

The morphology of electrospun fibers based on copolymers A and B, under the same spinning parameters, was compared. In the SEM images in Figure 1 it is clear that the different composition and structure of the copolymers (see materials) highly influence the microstructure and morphology of the electrospun samples. The A copolymer presents much thicker fibers as compared to B copolymer [Fig. 1(a,b)]. Furthermore, A copolymer fibers appear curly and flexible while B copolymer fibers look more straight and entangled. In B copolymer mats, there are also areas in which the fibers seem to bundle and form star-like structures, appearing bright (as indicated by the arrows). At a higher magnification [Fig. 1(c,d)], the difference in fiber diameters between the two electrospun materials is more evident. Web of A copolymer presents fiber diameters in the range of 1–3 μm and only very few submicron fibers, while for B copolymer, most of the fibers are below 1 μm in diameter. For B copolymer, ellipsoidal beads can be noticed together with aggregates, with the last once appearing bright. The nature of the B copolymer mesh suggests an unstable electrospinning jet, which for instance could be due to too low viscosity of the B copolymer solution. Electrospinning occurs, in fact, as a balance between surface tension, electrostatic, and viscous forces. Surface tension tries to reduce surface area by making spheres, and electrical forces attempt to achieve the least

charge density by increasing the surface area (promoting jet formation) while viscous forces determine the ease for solid fiber formation.[27–29] The higher the viscosity, the higher the electrical forces have to be to promote rapid changes in shape. With high viscosity, diameter reduction of the jet is not favored, leading to thicker fibers.[29] However, if viscous forces are too low, capillary breakup and unstable jet occur, and that results in a beaded morphology or even electrospraying if viscous forces are much lower than surface tension.[30] The fine jet is pulled out of the needle when the voltage surpasses a threshold value, and electrical forces overcome both surface tension and viscous forces. The jet is then accelerated by the electrostatic force following almost a straight line. Meanwhile, the solvent evaporates and the viscous resistance becomes more and more important, decelerating the thread movement. When jet acceleration becomes very small, any perturbations by air will change its straight movement and promote jet oscillation (simple pendulum analogy), giving rise to whipping, which dramatically thins the jet.[27,28,31,32]

The bright and star-like areas detectable in Figure 1(b,d) are shown at a higher magnification in Figure 2, from which it is clear that those areas are constituted by fibers assembling into bundles. Moreover, evidences are gained that copolymer B fibers are straight and joint in several points. They also have no uniform diameter, since among a majority of submicron fibers, fibers of 1–2 μm in diameter are also found. It can be noticed that the diameter of each fiber changes along the fiber itself. Fiber bundles and uneven fibers have been discussed in a study by Deitzel et al.,[33] where the irregularity in morphology with variation of diameter along the single fiber was attributed to low concentration of the spun solutions, which was also found to promote bead formation in the nonwoven sheet.[33,34] The low concentration generates low viscosity and consequently low viscous forces to balance the surface tension, which promotes the formation of beads instead of smooth fibers attempting the reduction of the surface area.[35–38] In Figure 2 beads are in fact clearly visible, as evidenced by arrows. Fiber bundles and beads both suggest that, at the adopted concentration of the solution, the electrospinning is occurring on the edge of the process windows. In particular, the uneven nature of single fibers could be an indication of rapid changes of viscosity when the solution flows into the needle. In fact, as shown in various studies, the polymer concentration, which is affecting the solution viscosity,[39] is a major parameter responsible for the fiber diameter.[5,9,33,40-47] The rapid viscosity (concentration) changes could be due to phase-separation phenomena suggested by the milky appearance of copolymer B solution.[48,49]

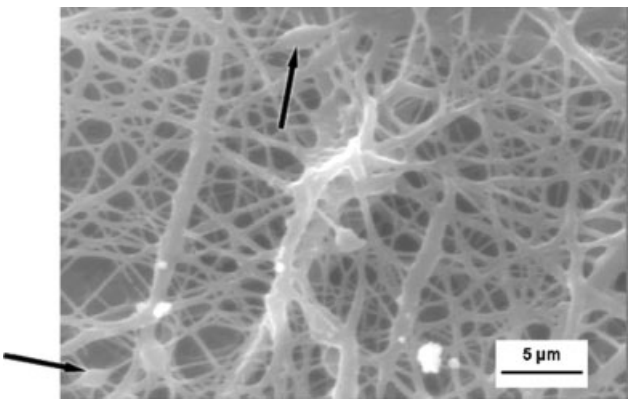

Figure 2 SEM image of electrospun B copolymer fibers (spinning voltage = 15 kV and DTC = 15 cm) focused on bright areas discussed in Figure 1. Magnification, ×3500.

The viscosity measurements showed that the solution containing A copolymer at 5% w/v concentration had a viscosity of 13.0 mPa s while B copolymer at the same concentration displayed a value of 5.5 mPa s. This result might be a consequence of different polymer–solvent interactions, because of different amount of the components, hydrophilicity (soft segment length), and molecular weight of the samples. The measurement may confirm, as hypothesized earlier, that bundles and beads in electrospun B copolymer could be derived from a too low viscosity (polymer concentration) of the solution.[33]

The mechanical test was performed on samples of A copolymer, electrospun at an SV of 20 kV and a DTC of 20 cm and of B copolymer, obtained with an SV of 25 kV and a DTC of 15 cm. The nonwoven sheets presented very similar morphology to those shown in Figures 1 and 2. The electrospun webs of A copolymer showed a stress and elongation at break 7–8 times higher than B copolymer meshes (4.1 ± 0.16 MPa versus 0.58 ± 0.05 MPa), while the elastic modulus did not present significant differences (1.11 ± 0.12 MPa versus 0.84 ± 0.24 MPa). The higher molecular weight of A copolymer and its different fiber web morphology, as compared to B copolymer, could explain the much higher elongation and stress at break recorded for A copolymer meshes, even though soft segment length in the polymer backbone is about half as long than that of B copolymer. As also shown in Figures 1 and 2, A copolymer fibers have a more curly appearance and intuitively are more suitable for high deformation than B copolymer fibers, where their degree of entanglement together with their straight character do not allow the web to deform as much as A copolymer webs.

The mechanical behavior of the two electrospun materials is linear elastic until 1/3 or 1/4 of the deformation at break is reached. After that, the curve slightly deviates from linearity and a knee-shaped

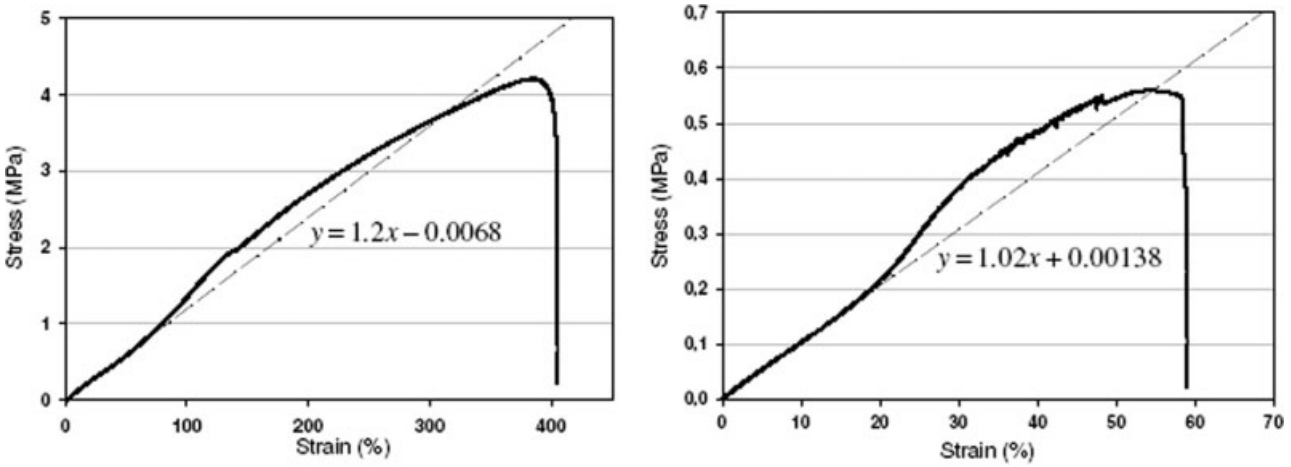

Figure 3 Mechanical properties of A copolymer (left) and B copolymer (right) electrospun webs. The linear regression curve (dashed line) was used to calculate the elastic modulus by means of the equation shown. The angular coefficient represents the value of the elastic modulus (in MPa).

region follows (much more pronounced for copolymer B because of the different scale). The end of the knee is likely the point where all the fibers are more or less aligned in the direction of the pulling force. Afterwards, a region with a lower modulus is visible (again more for copolymer B), indicating that gradual and progressive fracture of fibers occurs until the sample fails (Fig. 3). The webs mechanical characteristics could be explained looking at the fiber's bonding. The initial linear part of the curve is due to the network behavior: the fibers rearrange their relative position in the network as the constraints due to the fiber bonding allow. The knee-shaped region that follows is caused by the alignment and loss of mobility of the fibers in the network; thus, the samples become more rigid. The stretching of the single fibers is then responsible for the third (last) part of the curve.

Influence of process parameters on electrospun A copolymer

In Figure 4 the influence of applied voltage and DTC on fiber morphology is examined for A copolymer, when two different sets of parameters are employed. Looking at Figure 4(a,b) it is noticed that there is indeed no significant change in fiber morphology and diameter when both DTC and SV are increased. Fibers electrospun at higher voltage and DTC appear however a little curlier. This could be due to the fact that, in this second case, when DTC is higher, the fibers experience more cycles of bending instability (each one at a smaller scale than the previous one) and so they tend to coil and loop more.[50] The fiber elongation and associated thinning can continue as long as the charge on the jet supplies enough force, but the elongational viscosity continuously increases as the jet dries and, when the jet solidifies, the elongation stops.[50] In the case of this copolymer, the similarity in fiber diameter suggests that the two different combinations of parameters employed do not result in any significant difference in the elongation and thinning process. In Figure 4(c,d), the higher magnification allows for a better comparison of the diameter of the fibers. A common characteristic of these webs is that, together with a high majority of fibers with diameter around 2 μm, also a very few submicron fibers (as indicated by the arrows) are visible, especially in Figure 4(d). The presence of much thinner fibers together with thicker ones has no clear explanation yet, although in some cases,[3,50] it is claimed to be a consequence of the observed phenomena of "jet splaying."

Influence of applied voltage on electrospun B copolymer

In Figure 5, web morphology of B copolymer electrospun samples at different spinning parameters is shown by comparing [Fig. 5(a,b)] the micrographic images recorded at low magnification when voltage is increased at a parity of DTC. It can be noticed that the bright areas are more frequent but with lower propensity to stick out when a higher SV is employed and the fiber morphology is different. At higher magnification, significantly thicker fibers among a majority of submicron fibers are noticed, especially when SV is equal to 20 kV and DTC to 15 cm [Fig. 5(c)]. The average diameter of the fibers, obtained at higher SV, is somewhat higher than that recorded at lower SV. In both cases, the fibers appear to flatten and join in several points, and this may indicate that they are still solvent-wet when reaching the collector.[3] The explanation of a larger diameter, when the voltage is increased, at parity of DTC, is not straightforward, since in literature is

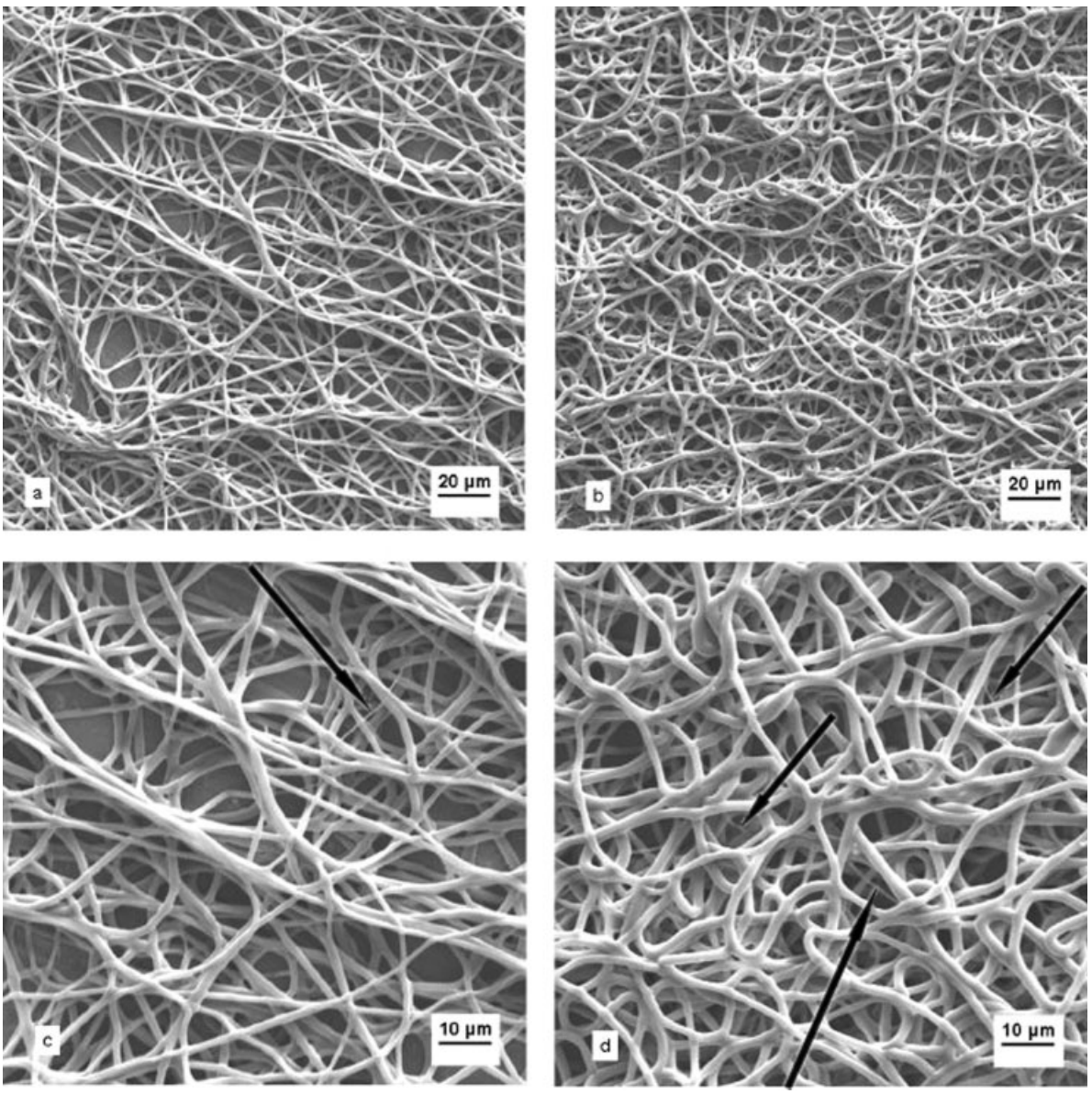

Figure 4 SEM images of electrospun webs from A copolymer 5% w/v concentration solutions in dichloromethane at different spinning parameters. (a) Spinning voltage (SV) = 15 kV, DTC = 20 cm, ×500; (b) SV = 30 kV, DTC = 30 cm, ×500; (c) SV = 15 kV, DTC = 20 cm, ×1000; (d) SV = 30 kV, DTC = 30 cm, ×1000.

disputable whether a higher applied voltage results in thicker fibers (because more fluid is ejected),[51] thinner (because of an increased jet elongation),[40] or basically it does not have any dominant effect compared to other parameters in determining fiber morphology.[47]

CONCLUSIONS

Electrospun fibers from biodegradable block copolymers, with different content and molecular weight of single components (PEG and PCL), proved to significantly differ in terms of single fiber diameter as well as morphology of nonwoven sheets produced. Fibers with curly and flexible appearance as well as fibers with straight and nonflexible appearance were generated, depending on the chemical nature of copolymer. In addition, chemical nature of copolymer also influenced the fiber density, such as assembles/bundles of fibers. In contrast to molecular weight and composition of copolymer, the process conditions (SV and DTC) during electrospinning showed little influence on the fibers formed. The different morphology of the two types of meshes proved to influence the mechanical properties of the two electrospun copolymers significantly. Block copolymers could be used in several applications, because a wide range of properties may be obtained upon changing the chemical composition and molecular weight of the single elements. This opens many possibilities for the biomedical field, where different

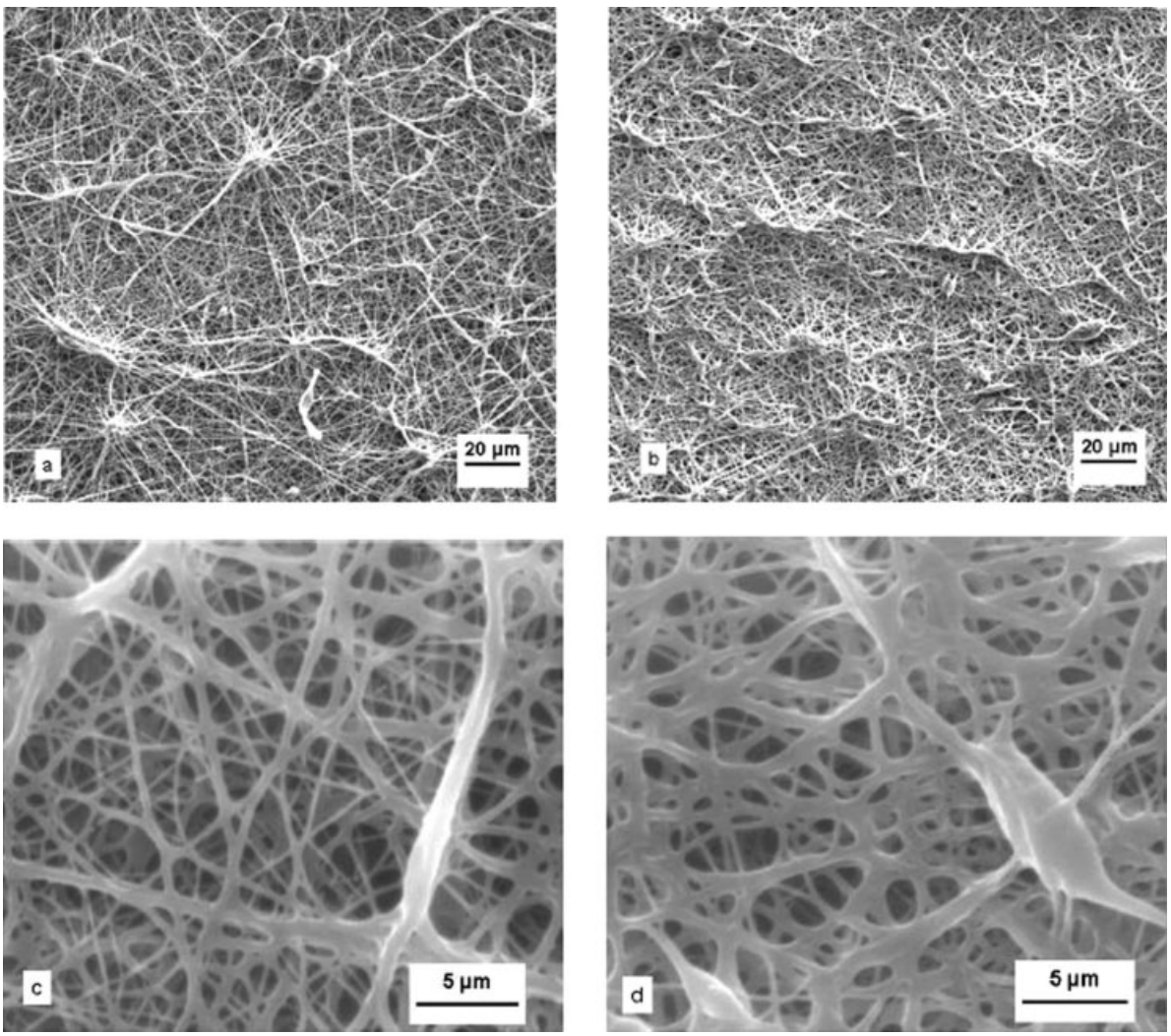

Figure 5 SEM images of electrospun B copolymer 5% w/v concentration solution in dichloromethane at different spinning conditions. (a) SV = 20 kV, DTC = 15 cm, ×500; (b) SV = 30 kV, DTC = 15 cm, ×500; (c) SV = 20 kV, DTC = 15 cm, ×3500; (d) SV = 30 kV, DTC = 15 cm, ×3500.

characteristics are required depending on the area of application of the medical device: prosthesis, filtration membrane, drug-delivery system, or tissue-engineered scaffold.

References

1. Baumgarten, P. K. J Colloid Interface Sci 1971, 36, 71.
2. Formhals, A (Schreiber-Gastell, Richard). US Pat. 2,109,333 (1938).
3. Reneker, D. H.; Chun, I. Nanotechnology 1996, 7, 216.
4. Kessick R.; Fenn, J.; Tepper G. Polymer 2004, 45 2981.
5. Doshi, J.; Reneker, D. H. J Electrostatics 1995, 35, 151.
6. Doshi, J. PhD Thesis, Akron University 1994.
7. Pedicini, A.; Farris, R. J. Polymer 2003, 44, 6857.
8. Shin, Y. M.; Hohman, M. M.; Brenner, M. P.; Rutledge, G. C. Appl Phys Lett 2001, 78, 1149.
9. Li, D.; Xia, Y. Adv Mater 2004, 16, 1151.
10. Yang, A.; Sun, K.; Wu, R. Gaofenzi Tongbao 2000, 2, 52.
11. Schaefer, K.; Thomas, H.; Dalton, P.; Moeller, M. Nanofibres for the production of multifunctional barrier structures. DWI Reports 2005, 129 (32. Aachener Textiltagung, 2005); p 10 schaefer/11.
12. Casper, C. L.; Yamaguchi, N.; Chase, B.; Rabolt, J. F.; Kiick, K. L. PMSE Prepr 2004, 91, 1030.
13. Stachurek, I.; Pielichowski, K. In Modern Polymeric Materials for Environmental Applications First International Seminar, Krakow, Poland, Dec 16–18, 2004; Vol. 1, p 137.
14. Gan, Z.; Jim, T. F.; Li, M.; Yuer, Z.; Wang, S.; Wu, C. Macromolecules 1999, 32, 590.
15. Choi, C.; Chae, S. Y.; Kim, T.-H.; Jang, M.-K.; Cho, C. S.; Nah, J.-W. Bull Korean Chem Soc 2005, 26, 523.
16. Pospiech, D.; Haeubler, L.; Meyer, E.; Janke, A.; Vogel, R. J Appl Polym Sci 1997, 64, 619.
17. Pospiech, D.; Haussler, L.; Eckstein, K.; Komber, H.; Voigt, D.; Jehnichen, D.; Friedel, P.; Gottwald, A.; Kollig, W.; Kricheldorf, H. R. High Perform Polym 2001, 13, S275.
18. Pospiech, D.; Haubler, L.; Meyer, E.; Jehnichen, D.; Janke, A. Design Monom Polym 1998, 1, 103.
19. Pospiech, D.; Häußler, L.; Eckstein, K.; Voigt, D.; Jehnichen, D.; Gottwald, A.; Kollig, W.; Janke, A.; Grundke, K.; Werner, C.; Kricheldrof, H. R. Macromol Symp 2001, 163, 113.

20. Adhikari, R.; Buschnakowski, M.; Lebek, W.; Godehardt, R.; Michler, G. H.; Calleja, F. J. B.; Knoll, K. Polym Adv Technol 2005, 16, 175.
21. Wnek, G.; Bowlin, G. L.; Simpson, D. G. Abstracts of Papers, 227th ACS National Meeting, Anaheim, CA March 28 to April 1, 2004; abstract no. CHED-655.
22. Martin, G. E.; Cockshott, I. D.; Fildes, F. J. (Imperial Chem Industries Ltd., UK). In Application GB/GB 19740034338 19740805, 1978; p 7.
23. Groitzsch, D.; Fahrbach, E. (Freudenberg, Carl, K.-G.; Fed Rep Ger). In Application: DE/DE, US Pat. 4,618,524, 1986; p 30.
24. How, T. V.; Clarke, R. M. Journal of Biomechanics 1984, 17, 597.
25. Martin, G. E.; Cockshott, I. D.; McAloon, K. T. (Imperial Chem Industries Ltd., UK). In Application: ZA/ZA, US Pat. 4,127,706, 1976; p 40.
26. Hutmacher, D. W. J Biomater Sci Polym Ed 2001, 12, 107.
27. Qin, X.-H.; Wan, Y.-Q.; He, J.-H.; Zhang, J.; Yu, J.-Y.; Wang, S.-Y. Polymer 2004, 45, 6409.
28. He, J.-H.; Wu, Y.; Zuo, W.-W. Polymer 2005, 46, 12637.
29. Krishnappa, R. V. N.; Desai, K.; Sung, C. J Mater Sci 2003, 38, 2357.
30. McKee, M. G.; Wilkes, G. L.; Colby, R. H.; Long, T. E. Macromolecules 2004, 37, 1760.
31. He, J.-H.; Wan, Y.-Q.; Yu, J. Y. Int J Nonlin Sci Num Sim 2004, 5, 243.
32. Fridrikh, S. V.; Yu, J. H.; Brenner, M. P.; Rutledge, G. C. Phys Rev Lett 2003, 90, 144502.
33. Deitzel, J. M.; Kleinmeyer, J.; Harris, D.; Beck Tan, N. C. Polymer 2000, 42, 261.
34. Fong, H.; Chun, I.; Reneker, D. H. Polymer 1999, 40, 4585.
35. Xu, H.; Yarin, A. L.; Reneker, D. H. Abstracts of Papers, 226th ACS National Meeting, New York, NY, September 7–11, 2003; abstract no. POLY-456.
36. Zuo, W.; Zhu, M.; Yang, W.; Yu, H.; Chen, Y.; Zhang, Y. Polym Eng Sci 2005, 45, 704.
37. Boland, E. D.; Pawlowski, K. J.; Barnes, C. P.; Simpson, D. G.; Wnek, G. E.; Bowlin, G. L. ACS Symp Ser 2006, 918, 188.
38. Carretero Gonzalez, J.; Barroso Bujans, F.; Lallave Rivas, M.; Barrero, A.; Gonzalez Loscertales, I.; Lopez Manchado, M. A. Revista de Plast Modernos 2006, 91, 551.
39. Phillies, G. D. J. Macromolecules 1995, 28, 8198.
40. Lee, J. S.; Choi, K. H.; Ghim, H. D.; Kim, S. S.; Chun, D. H.; Kim, H. Y.; Lyoo, W. S. J Appl Polym Sci 2004, 93, 1638.
41. Demir, M. M.; Yilgor, I.; Yilgor, E.; Erman, B. Polymer 2002, 43, 3303.
42. Kim, S.-H.; Green, R. E.; Kim, S. H. PMSE Prepr 2004, 91, 527.
43. Lu, Z.; Yan, W. Gaofenzi Tongbao 2005, 2, 35.
44. Kim, Y.; Lee, D. Y.; Lee, M.-H.; Lee, S.-J. J Korean Ceram Soc 2006, 43, 203.
45. Lee, B.; Lee, K.; Lee, D.; Pak, B.; Kim, H. J Korean Fiber Soc 2003, 40, 341.
46. Jun, Z.; Hou, H.; Schaper, A.; Wendorff, J. H.; Greiner, A. e-Polymers 2003, paper no. 9.
47. Tan, S. H.; Inai, R.; Kotaki, M.; Ramakrishna, S. Polymer 2005, 46, 6128.
48. Takemura, A.; Tomita, B.; Mizumachi, H. J Appl Polym Sci 1986, 32, 3489.
49. Grillo, I. Colloids Surf A Physicochem Eng Aspects 2003, 225, 153.
50. Reneker, D. H.; Yarin, A. L.; Fong, H.; Koombhongse, S. J Appl Phys 2000, 87, 4531.
51. Huang, Z.-M.; Zhang, Y. Z.; Kotaki, M.; Ramakrishna, S. Compos Sci Technol 2003, 63, 2223.